Journal of Japan Society of Civil Engineers, Ser.
B1 (Hydraulic Engineering), Vol. 70, No. 4, I_49-I_54, 2014.

INTERDEPENDENCE BETWEEN FLOW PATTERN, GEOMETRY AND FLUSHING EFFICIENCY OF IN-GROUND STILLING BASIN

M. E. MESHKATI SHAHMIRZADI[1], Tetsuya SUMI[2], Sameh A. KANTOUSH[3]

[1]Member of JSCE, Ph.D. Student, Disaster Prevention Research Institute, Kyoto University (Gokasho, Uji, Kyoto 611-0011, Japan)

[2]Member of JSCE, Professor, Disaster Prevention Research Institute, Kyoto University (Gokasho, Uji, Kyoto 611-0011, Japan)

[3]Associated Professor, Civil Engineering Department, The German University in Cairo (New Cairo City, Main Entrance of Al-Tagamoa Al-Khames, Cairo, Egypt)

This paper investigates the interaction between flow patterns and geometry of in-ground stilling basin (ISB) and its influence on flushing efficiency from ISB. The main governing parameters in our study were the normalized ISB length, drop number, normalized end-sill geometry (height and width), and Froude number. Using large scale particle velcocimetry, we classified the flow patterns into four groups of B-jump, U-jump, Periodic and Steady submerged jump. We found the favorable flow pattern has a positive correlation with drop number, while a negative correlation with relative ISB length. Moreover, the lateral free spaces of the end-sill do not increase the chances for sediment to be flushed out from ISB.

Key Words: *Flow patterns, hydraulic jumps, flushing efficiency, in-ground stilling basin.*

1. INTRODUCTION

Design of dissipater structures below flood mitigation dams (FMDs) still face a number of issues. Included amongst them are; low energy dissipation due to the effect of sediment deposition, and interruption in fish and sediment passage due to the presence of a tall and continuous end-sill.

One solution was suggested by MCD (Miami Conservation District, USA)[1)] to dig out the apron of the stilling basin creating a pool-shape stilling basin below FMDs. This type of stilling basin is called an in-ground stilling basin (ISB), which potentially can facilitate migration of aquatic animals[2)]. Although digging out the ground to create ISB is costly, by deepening the stilling basin we may are allowed to shorten the height of end-sill. A shorter end-sill height may compensate significant portion of the cost for deepen stilling basin.

An additional proposal investigated in the present study is to consider free spaces at both lateral sides of the end-sill to create a passage for fish and sediment which could be an eco-friendly alternative for a common continuous end-sill. It may increase the transparency of the FMD in terms of both sediment supply and fish migration. **Fig. 1** illustrates a conceptual schematic view of the ISB downstream of a typical FMD.

There are an enormous number of studies in literature devoted to the hydraulic characteristics of flow and sediment within stilling basins. These studies mainly concern, firstly, the occurrence of hydraulic jumps within a confined area; and secondly, control of the position of hydraulic jumps within it by: a) adding appurtenances e.g. sills, baffle blocks and an end-sill [3, 4)] and b) modifying the stilling basin structural design e.g. rise in bed level (positive step), abrupt drop in bed level (negative step), enlargement in bed width (gradual or sudden) and rough bed [5,6, 7)].

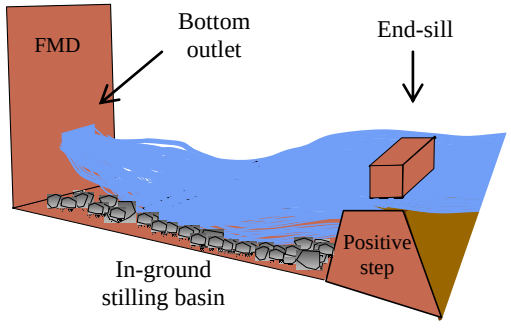

Fig. 1 Schematic view of in-ground stilling basin (ISB) below FMD.

Based on the literature review it was found that, a lack of information exists on the combination of a forced hydraulic jump with a simultaneous presence of a sudden enlargement and an abrupt drop. A forced hydraulic jump within a confined and complex structure such as an ISB has yet to be solved in the literature and still future studies are needed. Moreover, considering two free spaces at both sides of the end-sill in the presence of a movable bed increases the complexity of the phenomenon. This study focuses on a small expansion ratio (k=bottom outlet width/stilling basin width) of stilling basin equal to 0.2, as it is more practically common and causes a periodic and unstable flow pattern rather than larger expansion ratios[8].

The major objectives of this paper are: a) to evaluate the interaction between flow patterns, geometry and flushing efficiency of ISB under different hydraulic and geometrical conditions. b) to deeply clarify the effect of end-sill height and free spaces at both sides of the end-sill on the performance of ISB in the presence of movable sediment. The results were tabulated in terms of statistical measures and also illustrated through scatter plots.

2. MATERIALS AND METHODS

(1) Experimental setup

A scale model of stilling basin is constructed at Disaster Prevention Research Institute, Kyoto University. This scale model is based on the Froude similarity of prototype stilling basins downstream of three famous FMDs in Japan. The scale ratio of length in this study is 1/40. **Fig. 2** introduces the main governing parameters that govern the energy dissipation process within an in-ground stilling basin.

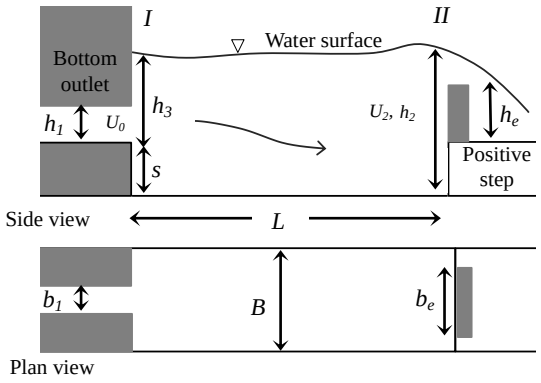

Fig. 2 Schematic side and plan view of the in-ground stilling basin (ISB) and the main governing parameters.

(2) Experimental measurement

The basic data collection procedure was the same for all of the experiments run. A water level meter was used to measure the water depth and its fluctuation throughout ISB. The sampling frequency for water level meter was set to 50 H_Z. Using an electro-magnetic current meter the 3D component of velocity was measured in different transversal and longitudinal cross sections for each test run. Moreover, for each test digital photographs were taken from side and plan view of ISB and visual observations were recorded using high resolution digital camera.

(3) Experimental condition

Extensive numbers of experiments were carried out under different geometrical and hydraulic conditions as: ISB length (L= 75, 100 and 125 cm), step depth (s= 5, 10 and 15 cm), different geometry of end-sill with various heights (h_e= 0, 4, 8, 12 and 13.5 cm) and various widths (b_e= 50, 40, 30, and 20 cm) has been examined. However, the width of ISB itself for all experiments was the same B= 50 cm equal to the width of flume.

For each ISB geometry configuration, In addition to the three different Froude number of supercritical flow at the bottom outlet (namely Fr_1= 2.8, 4.9 and 5.1), only one dimension of bottom outlet (h_1= 5 cm and b_1= 10 cm) was examined, thus, creates an expansion ratio of k=0.2 (k=b_1/B), similar to the average practical expansion ratio for FMDs. **Table 1** shows the experimental condition considered in the present study.

Table 1 Experimental condition.

$K=b_1/B$	L/B	s/h_1	h_e/h_c	$1-(b_e/B)$	Fr_1
0.2	1.5	1-3	0-4	0-0.6	2.8-5.1
	2	1-3	0-4	0-0.6	2.8-5.1
	2.5	1-3	0-4	0-0.6	2.8-5.1

3. RESULTS AND DISCUSSION

(1) Possible flow patterns within ISB

The frequently observed flow patterns within ISB can be summarized into four major families as: B-jump, U-jump, Periodic submerged jump and Steady submerged jump. The definition of the different jumps observed in current study is well described in the past[9]. The previous publication of the authors concerned about the classification of flow patterns within ISB; where it was noted that the type of hydraulic jumps within ISB is less dependent to Froude number at the face of bottom outlet, Fr_1, and more dependent on the end-sill height at the end downstream of ISB, h_e [10]; similar findings were reported by Kantoush et al. [4] and Ohtsu et al. as well [5].

(2) Flow Pattern Visualization using LSPIV

Large-scale particle image velocimetry (LSPIV) was used to evaluate the variation of flow velocities on the surface of flow within ISB using flow manager software. A digital camera is used to record images. White particles and light sources were used for velocity measurements.

Fig. 3a-c illustrates the time average surface velocity pattern obtained from LSPIV for U-jump, Periodic submerged jump and Steady submerged jump respectively. The velocity distribution spectrum in this figure is from dark black to bright white, where, the dark black indicates high negative velocities and bright white shows the area with higher positive velocities. The velocity vectors are depicted by green arrows and the gray lines on the plots are representative of the velocity contours on the surface of the flow.

In the case of a relatively short end-sill height and long ISB length, a narrow and symmetric super critical current is observed along the centerline of the ISB and creates V-shaped steady waves at the water surface, in which the roller fronts are continuously undulating over the stagnant water within ISB (U-jump). The toe of the jump in this flow pattern is located close to the bottom outlet (left-hand side of **Fig. 3(a)**). A further increase in end-sill height, or decrease in ISB length leads to submergence of the bottom outlet, in which, the wall above the bottom outlet obstructs the jump to move upstream. The submerged jumps observed in the present research were mostly periodic submerged jumps and steady-asymmetric submerged jump[8] **(Fig. 3(b)** and **(c)**).

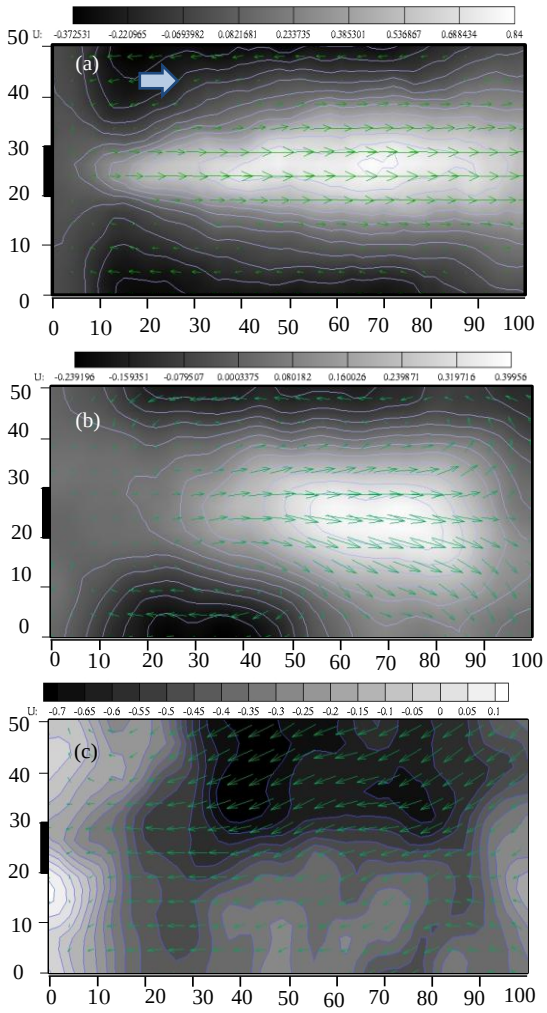

Fig. 3 Stationary flow field by using LSPIV; a) U-jump in presence of h_e=4 cm, b) Perio. Sub. Jump in presence of h_e=8 cm and c) Steady Sub. Jump in presence of h_e=12 cm, and all under following conditions L=100 cm, s=10 cm, b_e=50 cm and Q=15 l/s.

(3) ISB performance under fixed bed condition

a) Interdependence between flow pattern and ISB geometry

Herein, two flow pattern maps are presented based on the successful experimental data shown in **Table 1**. These flow pattern maps consist of both geometric and hydraulic parameters (**Fig. 4** and **5**). **Fig. 4** depicts the relationship between relative end-sill height, h_e/h_c, and relative ISB length, L/B, for all successful experimental data. In this figure, all four possible flow patterns within the ISB are shown. **Fig. 5** attempts to plot the possible flow patterns based on the relative end-sill height, h_e/h_c, versus the drop number, s/h_1.

The variation in drop number, s/h_1, and normalized ISB length, L/B, also showed a minor correlation with flow patterns within ISB. As it shown by dot line on **Fig. 4**, increasing the ISB

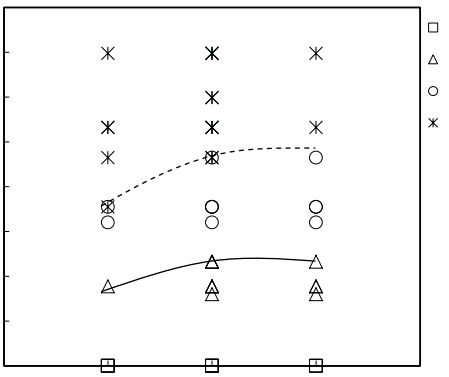

Fig. 4 The flow pattern map within ISB, concerning the normalized ISB length, L/B, and normalized end-sill height, h_e/h_c.

length negatively impacts on the stability of the flow. Moreover, increase in drop number, s/h_1, slightly improves the flow stability and allows us to shorten the end-sill height accordingly (**Fig. 5**).

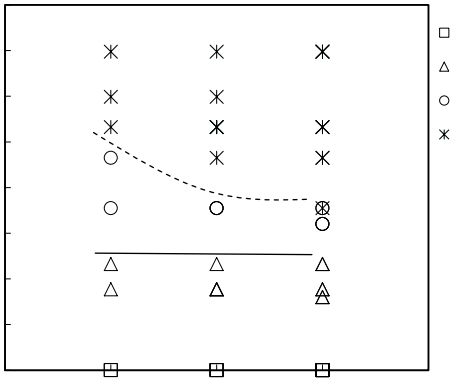

Fig. 5 The flow pattern map within ISB, concerning the drop number, s/h_1, and normalized end-sill height, h_e/h_c.

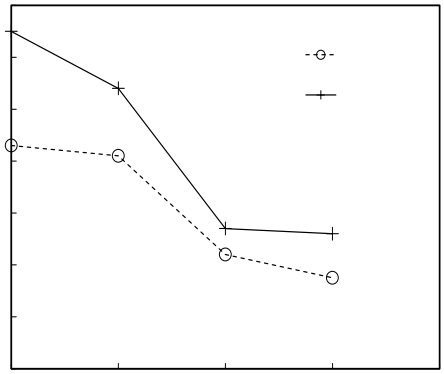

Fig. 6 The variation of normalized velocity reduction within ISB versus degree of end-sill width, $L/B=2$, $s/h_1=2$, $Fr_1=4.3$.

The previous publication of the authors [10] demonstrated that taller end-sill could induce the favorable flow patterns within ISB, which is submerged jump, and that is the most effective possible flow patterns in velocity reduction as well.

b) Effect of degree of free space and normalized end-sill height on velocity reduction

To clarify the effect of free spaces on velocity reduction two groups of tests are designed; in which all parameters were constant and only the end-sill width was varied. The first group of experiments concerned the effect of free spaces with a medium end-sill height (MMM: $h_e/h_c=1.8$) and the second group of experiments with a taller end-sill (MTM: $h_e/h_c=2.7$) (See in **Fig. 6**). The horizontal axis in **Fig. 6** shows the degree of end-sill width, 1-(b_e/B), in which b_e is the width of the end-sill and B is the width of the channel. The vertical axis is the normalized velocity reduction, U_0-U_2/U_0, between section *I* and *II*. U_0 is the initial outlet velocity and U_2 is the largest average velocity measured just upstream of end-sill. It is realized that decrease in end-sill width, negatively affects the velocity reduction within ISB, but considering a width of free space equal to 20% of channel width gives an almost equivalent performance to the no free space condition.

(4) ISB performance under movable-bed condition

To inspect the performance of ISB in the presence of movable sediment, all the parameters kept constant and only end-sill width, b_e, and end-sill height, h_e, varied. In total, eight experiments were designed as shown in **Table 2**. The experimental conditions consist of only on grain sizes of; sand gravel with diameter of 15 mm, uniform and non-cohesive. Preliminary tests showed that almost no more sediment with mean diameter of 3 to 7 mm was remained within ISB in less than half an hour after the experiment is started. Thus, we run the experiments with larger diameter of sediment. To find out the suitable diameter of sediment we used the scale factor of the sampled sediment obtained from Masudagwa stilling basin. The experiments with gravel are named SG1-8, in which the ISB was filled up with a thickness of 3 cm and each test was run for 1 hour to reach the equilibrium condition. Gravels flattered on the apron of stilling basin may provide a closer condition for ISB to the natural condition. Moreover, it could help to reduce the cost of protection works against abrasion.

Table 2 The designed variables to investigate the effect of height and free spaces at both sides of end-sill.

Exp. Case	h_e/h_c	1-(b_e/B)	d_{50} (mm)	Observed Flow Pattern
SG1	1.7	0	15	Steady Sub. jump
SG2	1.7	0.2	15	Perio. Sub. jump
SG3	1.7	0.4	15	U-jump
SG4	1.7	0.6	15	U-jump
SG5	2.6	0	15	Steady Sub. jump
SG6	2.6	0.2	15	Steady Sub. jump
SG7	2.6	0.4	15	U-jump
SG8	2.6	0.6	15	U-jump

a) Definition of flushing efficiency

If we define the flushing efficiency from ISB as illustrated in **Eq. 1**; by knowing the initial volume of sediment within ISB (V_i) before being exposed to discharge, and the final remained volume of sediment within ISB (V_f), we simply could realize the flushing efficiency.

$$FE = \left(\frac{V_i - V_f}{V_i}\right) \times 100 \quad (1)$$

b) Effect of free spaces on flow symmetry

Fig. 7(a) to **(d)** illustrates the final bed topography within the ISB for SG5-8. Having free spaces at both sides of end-sill resulted in a symmetric bed topography in equilibrium condition. While, in case of no free spaces (SG5), the bed topography in the equilibrium state was asymmetric. Presence of sediment deposition at the lateral side and within ISB confined the jump sideward. It eventually increases the expansion ratio, thus the possibility for having a symmetric flow pattern is higher as mentioned by Ohstu et al. [8)]

c) Effect of free spaces on bed abrasion pattern

By comparing **Fig. 7(a)** to **(d),** it can also be found that the larger free spaces caused larger sever erosion at the base of end-sill. For instance in SG7-8 the eroded area just upstream of end-sill is considerably large. Due to larger free spaces in SG7-8, the sequent depth of hydraulic jumps within ISB becomes much lower. Consequently, the type of jump from submerged jump changes to U-jump. U-jump hits the end-sill and positive step at ISB end. The reflection of flow from end-sill and positive step creates a large and strong vertical vortex just upstream of end-sill. This vortexes are the main reason for the sever abrasion just upstream of the end-sill. (See in **Fig. 7(a)** to **(d)**).

d) Effect of free spaces on flushing efficiency

In contrary with our expectations, the free space reduced the flushing efficiency of ISB. This fact comes from the interaction between the geometry of end-sill and the flow pattern. The wider the free space, the plunged jump into the ISB is less downward. As explained earlier, when the plunged jump into ISB is less downward, the reverse flow within ISB is much stronger. Thus, the sediment from the base of end-sill would transport upstream, then, the chance for sediment for being flushed out is very low (See in **Fig. 8**).

However, as can be seen in **Fig. 8**, there is an exception. In SG6 a greater flushing ratio has been observed rather than SG5. The flow pattern in case of SG5 is an asymmetric submerged jump, and it is oriented to the right side wall. It provides a big horizontal circulation system within ISB that carry the entire eroded sediment from right side-wall to the left sidewall and then deposit them there. Thus, the mount of sediment deposited is formed only in one side of the ISB. While, by considering a minimum free space (SG6) the flow pattern within ISB becomes symmetric. It causes to creation of two mounts just upstream of end-sill base. Therefore, more sediment can be flushed out from ISB in this case.

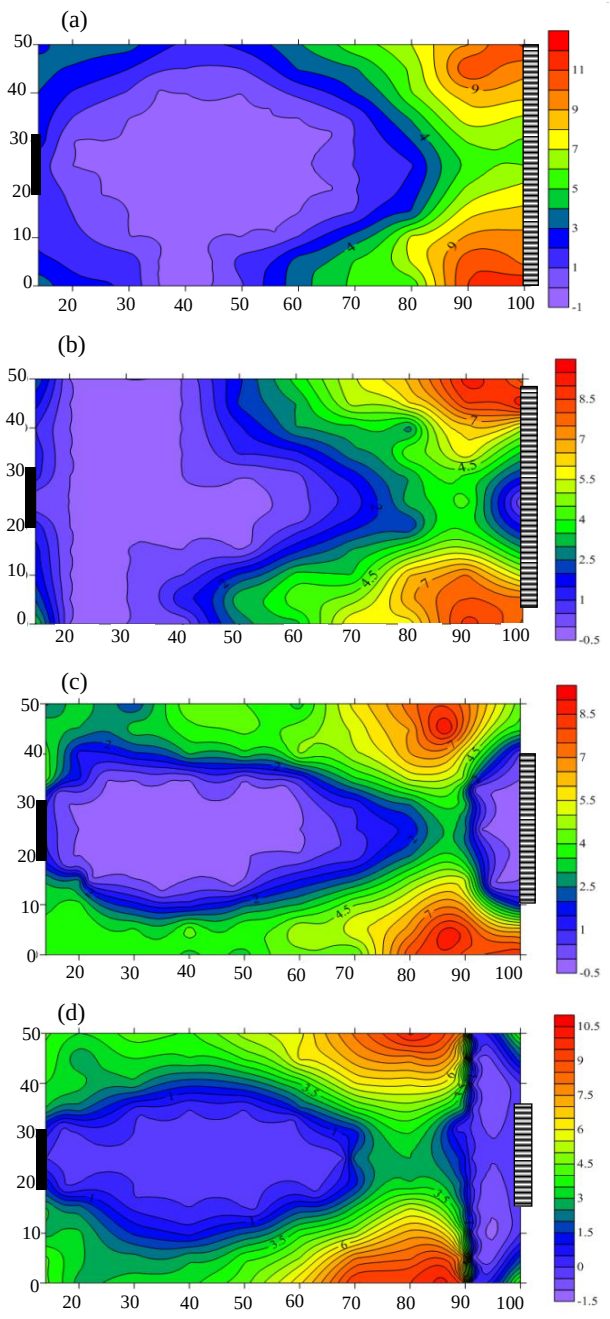

Fig. 7 The bed topography within ISB under h_e/h_c= 2.6; a) SG5: 1-(b_e/B)=0 , b) SG6: 1-(b_e/B)=0.2, c) SG7: 1-(b_e/B)=0.4 and d) SG8: 1-(b_e/B)=0.6.

We propose to avoid the asymmetric flow pattern within ISB, in particular when the expansion ratio, *k*, is small, by considering a minimum required free spaces at both side of end-sill we can positively provide a symmetric flow within ISB. Moreover, 32% increase in normalized end-sill height, h_e/h_c, positively leads to 12.5% increase in sediment flushing from in-ground stilling basin (see in **Fig. 8)**. It is also showed that the free space width is around 20% of the channel width has almost same performance regarding to velocity reduction with no free spaces condition (See in **Fig. 6**).

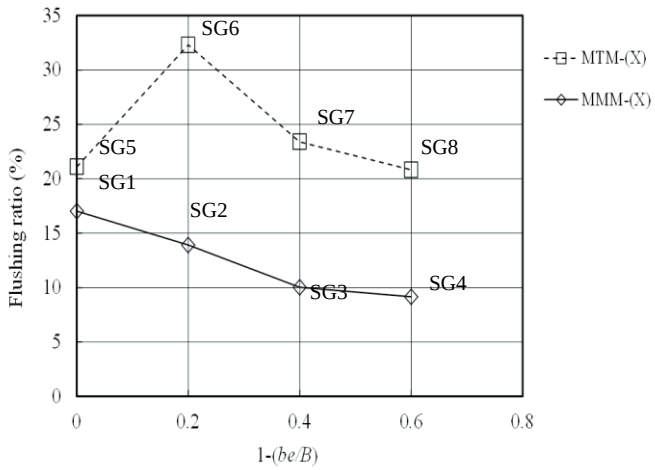

Fig. 8 Flushing efficiency ratio versus degree of free space for SG1-8.

f) Effect of end-sill height on flushing efficiency

We realized that a taller end-sill could finally result in a better performance for ISB regarding flushing (**Fig. 8**). This finding is in contrary with our first hypothesis as mentioned in the introduction of this paper. The main reason why a taller end-sill leads to a higher flushing ratio is that the taller end-sill induces a greater sequent depth resulting in a jump directed downwards into the ISB apron. When the jump hits the ISB apron, it cleans out all the sediment in the vicinity and transports it to the base of the end-sill. As shown earlier in these cases (**Fig. 7a**) this would form a mound just upstream of the end-sill. The sediment at the top of the mound has a higher chance to be flushed out from the ISB.

While, in case of a shorter end-sill (SG1-4), because of a lower sequent depth the jump is directed almost horizontal and hits the end-sill and positive step at the downstream end of the ISB, resulting in the creation of strong vertical circulations at the base of the end-sill. The consequence of these circulations along with intense reverse flow at the lateral sides of the ISB is to transport back all the sediment and deposit them at the lateral sides of ISB far from the end-sill, resulting in less chance for sediment to be flushed out.

CONCLUSION

Present study systematically investigates the influence of in-ground stilling basin (ISB) geometry on the flow and sediment flushing/deposition processes. It was found that geometrical parameters, such as end-sill height and ISB length, plays key role in defining the flow patterns within an ISB that then influence on its performance. Two universal flow pattern maps were proposed to ease the identification of flow patterns within an ISB under certain geometric and hydraulic conditions.

Through this experimental study we concluded that deepening the stilling basin allows us to slightly shorten the end-sill height. However, a taller end-sill provides better ISB performance with regard to both energy dissipation and flushing efficiency.

Furthermore, it was found that due to the small expansion ratio of the stilling basin, even in combination with a very tall end-sill, a periodic submerged jump with deflection is induced within the ISB. This type of flow is typically unfavorable for design purposes. But the experimental results evidence that, free lateral spaces at the end-sill can be utilized to stabilize the symmetry of flow.

Moreover, considering free spaces equal to 20% of channel width, provides other important advantages as higher flushing efficiency, a passage for fish, and improvement of the flow condition downstream of the ISB.

REFERENCES

1) Morgan, A.E.: The Miami Conservancy District, McGRAW-HILL BOOK COMPANY, 1951.
2) Sumi, T., Kantoush, S. A., and Shirai, A.: Worldwide Flood Mitigation Dams: Operating and Designing Issues. *The international symposium on urban flood risk management*, Graz, Austria, 2011.
3) Hager, W. H., and Bretz, V.N.: Hydraulic jumps at positive and negative steps, *Journal of hydraulic research*, Vol. 24, No. 4, pp. 237-253, 1986.
4) Hager W.H., Li D.: Sill-controlled energy dissipator. *Journal of Hydraulic Research*, 30(2): 165-181; 31(2),: 282-285, 1992.
5) Kantoush, S. A., Sumi, T., and Schleiss, A.: Geometry effect on flow and sediment deposition patterns in shallow basins, *Journal of Hydraulic Engineering*, JSCE, Vol.55, pp. 133-138, 2010.
6) Ohtsu, I., and Yasuda, Y.: Transition from supercritical to subcritical flow at an abrupt drop, *Journal of hydraulic research*, Vol. 29, No. 3, pp. 309-328, 1991.
7) Pagliara, S.: Influence of sediment gradation on scour downstream of block ramps, *Journal of Hydraulic Engineering*, Vol. 133, No. 11, pp. 1241-1248, 2007.
8) Ohtsu, I., Yasuda, Y., and Ishikawa, M.: Submerged hydraulic jumps below abrupt expansions, *Journal of hydraulic engineering*, Vol. 125, No. 5, pp. 492-499, 1999.
9) Ferreri, G.B., and Nasello, C.: Hydraulic jumps at drop and abrupt enlargement in rectangular channel, *Journal of hydraulic research*, Vol.40, No.4, pp.491-504, 2002.
10) Meshkati Shahmirzadi, M. E., and Sumi, T.: Hydraulic Design of In-ground Stilling Basin under Submerged Jump Condition in Flood Mitigation Dams, *Journal of Japan Society of Civil Engineering*, Vol. 69, pp. 79-84, 2013.

(Received September 30, 2013)